



**HAL**  
open science

## Measurement of absolute K X-ray emission intensities in the decay of $^{103m}\text{Rh}$

Jonathan Riffaud, Philippe Cassette, Didier Lacour, Valérie Lourenço, Isabelle Tartes, Mark Kellett, Margot Corbel, Marie-Christine Lépy, C. Domergue, C. Destouches, et al.

### ► To cite this version:

Jonathan Riffaud, Philippe Cassette, Didier Lacour, Valérie Lourenço, Isabelle Tartes, et al.. Measurement of absolute K X-ray emission intensities in the decay of  $^{103m}\text{Rh}$ . Applied Radiation and Isotopes, 2018, 134 (SI), pp.399-405. 10.1016/j.apradiso.2017.10.003 . cea-01803820

**HAL Id: cea-01803820**

**<https://cea.hal.science/cea-01803820>**

Submitted on 5 Jul 2023

**HAL** is a multi-disciplinary open access archive for the deposit and dissemination of scientific research documents, whether they are published or not. The documents may come from teaching and research institutions in France or abroad, or from public or private research centers.

L'archive ouverte pluridisciplinaire **HAL**, est destinée au dépôt et à la diffusion de documents scientifiques de niveau recherche, publiés ou non, émanant des établissements d'enseignement et de recherche français ou étrangers, des laboratoires publics ou privés.

# Measurement of Absolute K X-Ray Emission Intensities in the Decay of $^{103\text{m}}\text{Rh}$

J. Riffaud<sup>[1]</sup>, P. Cassette<sup>[1]</sup>, D. Lacour<sup>[1]</sup>, V. Lourenço<sup>[1]</sup>, I. Tartès<sup>[1]</sup>, M.A. Kellett<sup>[1]</sup>,  
M. Corbel<sup>[1]</sup>, M.-C. Lépy<sup>[1]</sup>, C. Domergue<sup>[2]</sup>, C. Destouches<sup>[2]</sup>, H. Carcreff<sup>[3]</sup>, O. Vigneau<sup>[4]</sup>

<sup>1</sup>*CEA, LIST, Laboratoire National Henri Becquerel (LNE-LNHB), CEA-Saclay 91191 Gif-sur-Yvette Cedex, France.*

<sup>2</sup>*CEA, DEN, DER, Laboratoire de Dosimétrie, Capteurs et Instrumentation (LDCI), Cadarache, 13108 Saint Paul-lez-Durance, France*

<sup>3</sup>*CEA, DEN, DRSN, Laboratoire de Support aux Programmes d'Irradiation (LSPI), CEA-Saclay 91191 Gif-sur-Yvette Cedex, France*

<sup>4</sup>*CEA, DEN, DEC, Laboratoire d'Analyses Radiochimiques et Chimiques (LARC), Cadarache 13108 Saint Paul-lez-Durance, France*

## Abstract

A new experiment was designed to measure the photon emission intensities in the decay of  $^{103\text{m}}\text{Rh}$ . The rhodium samples were activated in the ISIS experimental nuclear reactor at CEA Saclay. The procedure includes an absolute activity measurement by liquid scintillation counting using the Triple-to-Double Coincidence Ratio method, followed by X-ray spectrometry using a high-purity germanium detector to determine the photon emission intensities. The new result ( $I_X = 0.0825 (17)$ ) is derived with a significant reduction of the uncertainty.

**Keywords:**  $^{103\text{m}}\text{Rh}$ , TDCR method, X-ray spectrometry, Photon emission intensity, reactor dosimetry.

---

## 1. Introduction

The knowledge of the fluence and energy distribution of neutrons in a nuclear reactor is extremely important for the validation of neutron transport codes, with an application for assessing the reactor vessel aging. This is achieved through the use of so-called “dosimeters”

which are metal samples irradiated in the reactor core. These are irradiated and activated by the local neutron flux, prior to being extracted from their location. After irradiation, the dosimeters' activity is usually measured by gamma-ray spectrometry. From the activity value and irradiation information, it is possible to determine the neutron flux at the dosimeter location. There are many dosimeter types, each characterizing a specific neutron energy region. Rhodium is used for neutron fluence measurements in nuclear reactors since the inelastic scattering reaction  $^{103}\text{Rh}(n,n')^{103\text{m}}\text{Rh}$  is particularly useful to characterize the neutrons with energy around 1 MeV. Rhodium dosimeters are usually in the shape of a disk with 50- $\mu\text{m}$  thickness and 8-mm diameter and the activity measurement is performed by spectrometry of low-energy photons. Indeed,  $^{103\text{m}}\text{Rh}$  only de-excites by a highly converted transition (the gamma emission intensity is less than 0.1%) towards the ground state of  $^{103}\text{Rh}$  (Figure 1), leading to intense X-ray and Auger electron emission. However, perhaps due to its short half-life (56.115 (6) min (Nucleide, 2016)),  $^{103\text{m}}\text{Rh}$  has been very little studied, mostly around 1960-1970 and the last measurement of the X-ray emission intensity dates back to 1994 (Schötzig, 1994). Although the radioactive half-life is well known (with 0.01% relative uncertainty), this is not the case for the X-ray emission intensities. Indeed, they are specified with relative standard uncertainties between 5.5% and 7%. These high values have a direct impact on the activity measurements leading to relative standard uncertainties of more than 8%.

The main objective of this study is to measure the absolute X-ray emission intensities of  $^{103\text{m}}\text{Rh}$ , in order to improve the associated uncertainties. Due to the short half-life of this nuclide, we take advantage of the irradiation facility which is located close to the Laboratoire National Henri Becquerel, at the CEA Saclay research centre. This is achieved by preparing rhodium samples, which are activated by a neutron flux to produce  $^{103\text{m}}\text{Rh}$ , and specific sources for activity and spectrometry measurements. The activity is determined by liquid

scintillation counting (LSC) using the triple-to-double coincidence ratio (TDCR) method. The photon emission intensities are measured by X-ray spectrometry using a high purity germanium detector (HPGe) accurately calibrated in the low-energy range. Knowledge of the source activities makes it possible to derive absolute X-ray emission intensities. Each step is detailed hereafter and the experimental results are discussed in the last section.

## **2. Source preparation**

Due to the short half-life of  $^{103\text{m}}\text{Rh}$ , it is necessary to carefully select the experimental conditions and examine each step of the procedure to minimize the time, taking into account all constraints (radioprotection, chemistry) to obtain suitable samples for the activity and spectrometry measurements.

### ***2.1 Chemical constraints***

The first step is the production of  $^{103\text{m}}\text{Rh}$  by neutron activation from  $^{103}\text{Rh}$  – the only stable isotope of rhodium. The neutrons with energy about 1 MeV interact with rhodium by the inelastic scattering reaction producing  $^{103\text{m}}\text{Rh}$ . However,  $^{103}\text{Rh}$  also undergoes thermal neutron capture and forms  $^{104\text{m}}\text{Rh}$  and  $^{104}\text{Rh}$ , which have half-lives of 4.34 min and 42.3 s, respectively (Live Chart of Nuclides, 2017). The capture cross sections (Santamarina et al, 2009 and Zsolnay et al, 2012) are very high for thermal neutrons so a significant number of atoms of  $^{104\text{m}}\text{Rh}$  and  $^{104}\text{Rh}$  will be formed during irradiation. However, since the half-lives of these two radionuclides are very short, the measurements start after these two radionuclides have decayed.

Rhodium is a transition metal and a member of the platinum group, which due to its hardness, inalterability and electronic configuration, is chemically inert and weakly attacked by most acids. To prepare the metal sample, it is necessary to cope with two contradictory conditions:

(i): To irradiate rhodium in the reactor, it must be in the form of a metallic pellet,

(ii): For the liquid scintillation measurement the rhodium sample must be dissolved in solution.

Since all tests to dissolve a pure rhodium metallic pellet were unsuccessful, a compacted disk of pure rhodium powder was used for the irradiation and then ground further before the dissolution.

A specific dissolution protocol for the rhodium powder was established by the Laboratoire d'Analyses Radiochimiques et Chimiques (LARC) of CEA Cadarache. It has certain disadvantages, especially on the dissolution and retrieval times of the solution which are very long (more than 2h30), when compared to the  $^{103m}\text{Rh}$  half-life. Moreover, the loss of material due to grinding is not quantifiable and the colour of the solution after the dissolution is red, inducing undesirable colour quenching for the liquid scintillation measurement.

It is however possible to find rhodium in other compounds, e.g. rhodium(III) chloride ( $\text{RhCl}_3$ ). Rhodium chloride is a very dark red powdery crystalline solid in the form of a salt, which is soluble in water, thus allowing samples to be readily prepared for the measurements. However, rhodium chloride has also some drawbacks. Firstly, the chlorine is activated by thermal neutrons and  $^{36}\text{Cl}$  and  $^{38}\text{Cl}$  are created together with  $^{103m}\text{Rh}$ , producing additional activity during the liquid scintillation measurements. Secondly, the liquid solution of  $\text{RhCl}_3$  is opaque and has a dark red colour, which also induces colour quenching. And finally,  $\text{RhCl}_3$  is

corrosive and must therefore be enclosed in an airtight container before being immersed in the reactor core.

Finally, for this experiment it was chosen to use two kinds of rhodium samples: a compacted pellet of pure rhodium powder and  $\text{RhCl}_3$  powder, both purchased from Sigma-Aldrich Co. LLC., with respective mass purities of 99.95% and 99.98%.

## ***2.2 Irradiation***

The rhodium samples were irradiated at the experimental reactor ISIS of CEA Saclay which operates at a maximum power of 700 kW with a fuel based on uranium silicide. In order to have sufficient activity to obtain good counting statistics during the liquid scintillation and spectrometry measurements (i.e. a relative uncertainty in the full energy peaks less than 1%), it was calculated that the activity of the samples at the end of the irradiation must be at least 5 MBq. Thus, the optimum rhodium mass for irradiation was determined to be about 100 mg. However, only up to 50 mg of pure rhodium powder can be dissolved with the protocol, because the dissolution efficiency is not 100%. In the case of  $\text{RhCl}_3$ , the powder consists of 41.1% rhodium by mass. To obtain the equivalent of 100 mg of rhodium, it is thus necessary to irradiate 216 mg of  $\text{RhCl}_3$  powder. For the irradiation, the samples must be isolated from the water of the reactor pool and were arranged as presented in Figure 2. The  $\text{RhCl}_3$  powder is first poured into an aluminium case, then placed in a boron nitride housing, whose function is to filter the thermal neutrons in order to reduce the chlorine activation. The pellet of pure rhodium is placed under the aluminium case containing the  $\text{RhCl}_3$ , inside the boron nitride (BN) housing. Both are closed with clips to ensure air-tight seals, before being enclosed in a second aluminium housing with a screw lid and an aluminium gasket. The complete housing is then placed in a specially machined aluminium rod and introduced into an assembly which

is inserted into an irradiation channel in the ISIS reactor core. The samples are irradiated for 30 minutes with a reactor operating power of 10 kW.

### ***2.3 Chemistry and measurement sequences***

The two irradiated samples are processed in parallel for source preparation and activity and emission intensity measurements:

- i. First, the compacted powder pellet is measured by low-energy photon spectrometry while the  $\text{RhCl}_3$  is dissolved. The 216 mg of  $\text{RhCl}_3$  powder are mixed with the smallest volume of water required (600  $\mu\text{L}$ ) to dissolve them, which allows a minimal self-attenuation correction for the spectrometry measurements. From the solution of  $\text{RhCl}_3$ , five sources are prepared for liquid scintillation measurements. A small amount of water is also added to further stabilize the sources. After mixing with the scintillating cocktails, the source activity was measured by liquid scintillation counting. The remaining  $\text{RhCl}_3$  solution was poured into a container specially designed for the spectrometry measurement.
- ii. Second, as soon as the pellet spectrometry measurement is finished, it is taken for dissolution, while the  $\text{RhCl}_3$  solution is in turn measured by spectrometry. The pellet is dissolved according to the procedure established and validated before the irradiation and five sources are prepared for the liquid scintillation measurement, as in the case of  $\text{RhCl}_3$ . In addition, the sources of  $\text{RhCl}_3$  and pure rhodium are also measured by gamma-ray spectrometry to determine the impurities in the sources and estimate their activities.

## **3. Liquid scintillation counting**

After dissolution, one drop of the rhodium source was mixed with a commercial liquid scintillator (Ultima Gold AB) and some water, thus no problem of colour quenching was encountered for the measurement of the scintillating sources using the TDCR method. The measurements were made at LNHB using the locally-developed triple counter (Cassette and Vatin, 1992).

The detection efficiencies, in double and triple coincidences, are a function of the intrinsic light yield of the detector and can be calculated as a weighted sum of all individual efficiencies corresponding to the absorption of energy following the possible atomic rearrangements after the gamma transition. This includes the absorption by the scintillator of the energy of the conversion electrons, but also of the energies of the associated Auger electrons and X-rays (Table 1). For a large number of observed transitions, the ratio of triple to double detection efficiencies is assumed to be equal to the ratio of observed triple and double coincidences and this equality allows the determination of the intrinsic light yield of the scintillator, and thus the detection efficiency. The atomic rearrangement calculation is based on a simplified KLM model, i.e. without considering the L and M subshells and without distinction between the M and other outer shells. This assumption is justified by the low energy difference between the subshells (e.g. about 400 eV between the L1 and L3 binding energies) and also because the atomic rearrangements are coincident with the absorption of conversion electrons in the scintillator. Evaluation of the energy transfer of the ionising radiation to the LS-cocktail is obtained using the following assumptions:

- i. The Auger and conversion electrons are totally absorbed by the cocktail;
- ii. The XL emission is totally absorbed by the cocktail by photoelectric interaction;
- iii. The XK emission interacts with the LS-cocktail by Compton and photoelectric effects. The energy transferred to the cocktail is calculated using the Monte Carlo simulation code PENELOPE (Salvat et al., 2015).

The conversion of a gamma transition depends on the multipolarity of the transition, which is not well-established for  $^{103\text{m}}\text{Rh}$ . From the previously reported X-ray intensities, the multipolarity is between E3 and E3 + 0.08%M4. The influence on the internal conversion coefficient values, calculated using the BrIcc code (Kibédi, 2008), is presented in Table 2.

From these values, it can be observed that the differences in the conversion coefficients obtained with the two hypotheses on the multipolarity of the transition, are consistent within the associated uncertainties. Thus, the values used for determining the detection efficiency are the mean values of each data set with the associated standard deviations. The global uncertainty of the detection efficiency is calculated using a Monte Carlo method according to the Guide to the expression of Uncertainty in Measurement, supplement 1 (JCGM, 2008). By considering Gaussian fluctuations of the decay-scheme parameters and the Birks parameter,  $kB$ , and by considering the experimental fluctuations of the TDCR value, the relative standard uncertainty of the detection efficiency is 0.3 %. This is also the relative standard uncertainty of the activity of the solution, as the other uncertainty components (counting statistics and weighing) are negligible.

## **4. X-ray and gamma-ray spectrometry**

The  $^{103\text{m}}\text{Rh}$  emission intensities are measured by low-energy photon spectrometry. The reference efficiency calibration for point sources is determined experimentally and using Monte Carlo simulation. For the rhodium sample measurements, it was necessary to compute efficiency transfer factors to take into account the geometry change, since the measured samples are not point sources.

### ***4.1 Efficiency calibration***

The spectrometry measurements are performed with an N-type high-purity germanium (HPGe) detector. The planar germanium crystal is 15.44 mm in diameter and 11.1 mm thick with a dead-layer thickness of about 0.8  $\mu\text{m}$  and the beryllium window is 127  $\mu\text{m}$  thick. Two tantalum collimators are used to reduce scattering effects. The first one has an aperture diameter of 14 mm and is placed 1.2 cm from the germanium crystal and the second, with a 10 mm aperture diameter, at 7.1 cm from the germanium crystal, and thus close to the radioactive source. The experimental efficiency calibration is established using standard point sources for a reference geometry (source-to-detector distance: 7.8 cm) according to Eq.1:

$$\varepsilon(E) = \frac{N(E)}{I(E) A t} \prod_i C_i \quad (\text{Eq. 1})$$

where  $\varepsilon(E)$  is the detector efficiency at energy  $E$ ,  $N(E)$  is the number of counts in the full energy peak at energy  $E$ ,  $I(E)$  is the emission intensity of the line with energy  $E$ ,  $A$  is the activity (Bq) of the standard point source,  $t$  is the acquisition time (s) and  $C_i$  different correction factors (decay, coincidence summing, etc.).

$N(E)$  is obtained using the COLEGRAM software (Ruellan et al., 1996), which allows accurate fitting of the peak shapes with various mathematical functions (e.g. Gaussian, Voigt, Gaussian with tail, etc.). The peaks from a gamma emission are fitted with a Gaussian function and those from an X-ray emission are fitted using a Voigt function. The Gaussian width corresponds mainly to the statistics of electron-hole pair creations in the germanium crystal and the Lorentzian width of the Voigt function corresponds to the natural Lorentzian width of each X-ray line. In order to accurately determine the K X-ray emission intensities, the peak shape analysis takes into account the scattering effect (i.e. low-energy tailing).

A poly-logarithmic function is fitted to the experimental values using the least-squares method, in order to be able to obtain an efficiency value for any energy (Figure 3).

In addition, Monte Carlo simulations with GEANT4 (Agostinelli et al., 2003) and PENELOPE (Salvat et al., 2015) are used to refine the efficiency calibration curve due to the lack of standard sources in the required low energy range and also to compute the efficiency transfer factors (see §4.2). The detector geometry was simulated starting from the supplier's nominal specifications and the dimensions from the radiograph. The optimized dimensions are given in Table 3 and the Monte Carlo results are plotted and compared with the experimental ones in Figure 3. The data used for the Monte Carlo simulations in Table 3 for the crystal diameter and thickness and window-detector distance were measured on the radiograph of the detector and differ slightly to the supplier's nominal values. The HPGe crystal has three regions: one with pure Ge (active crystal), another with boron ions (dead-layer) and the last with lithium ions (inactive crystal). The boron and lithium ions have probably migrated since the time of construction of the detector, which explains the thickness of the inactive crystal, since the detector is more than ten years old.

#### ***4.2 Rhodium sample measurements***

The photon emission intensities of the rhodium samples were measured at the reference distance of 7.8 cm; the pellet was sandwiched between Mylar<sup>®</sup> films and the RhCl<sub>3</sub> solution was packed in a Plexiglas<sup>®</sup> container specially designed for the measurements. The emission intensities of <sup>103m</sup>Rh were derived as:

$$I(E) = \frac{N(E)}{\varepsilon(E) A t} \prod_i C_i \quad (\text{Eq. 2})$$

where the source activity  $A$  is determined from the liquid scintillation counting measurements.

An example of the K X-ray spectrum processing with COLEGRAM is shown in Figure 4. As already mentioned, the X-ray peaks are fitted using a Voigt function, with natural X-ray

widths fixed according to tabulated values (Campbell and Papp, 2001) and the tailing due to scattering is taken into account.

The main correction factors to be considered are:

- i. The half-life correction, which takes into account the radioactive decay between the reference date (when the source activity is measured) and the beginning of the acquisition,
- ii. The decay correction, which takes into account the radioactive decay during the measurement,
- iii. The self-attenuation correction, which takes into account the attenuation of the photons inside the sample volume,
- iv. The geometry correction, which takes into account the change in the source-detector distance between measurement and calibration,
- v. The solid angle correction, which takes into account the change of the solid angle of detection between measurement and calibration, since in this geometrical arrangement the measured samples cannot be considered as point sources.

Here the half-life and decay corrections are significant, due to the short half-life of  $^{103\text{m}}\text{Rh}$ . For this study, the last three factors were determined simultaneously with Monte Carlo simulations using both PENELOPE and GEANT4 particle transport codes. For this we compare the efficiency obtained for a point source (see §4.1) with the efficiency for volume sources having the size of the  $\text{RhCl}_3$  source and the pellet. Thus, the efficiency transfer factor, which corresponds to the ratio of these two efficiencies, takes into account the self-attenuation and the geometry and solid angle changes. The calculation was performed using the two codes which provided consistent results. The uncertainty is estimated from the result change induced

by small variations of the source dimensions and by the statistical uncertainty that was less than two percent.

To help determine the transition multipolarity, we also measure the gamma-ray emission intensity despite its very low value, estimated to be 0.069%.

### ***4.3 Gamma-emitting impurities***

Gamma-ray spectrometry was performed using a larger coaxial HPGe detector (100 cm<sup>3</sup>) calibrated in the 50-1800 keV range to check the impurities, in order to determine their possible influence on the X-ray emission intensities. The impurities observed during the measurements are: <sup>24</sup>Na: 1.5 Bq.g<sup>-1</sup>; <sup>38</sup>Cl: 14 Bq.g<sup>-1</sup>; <sup>82</sup>Br: 4 Bq.g<sup>-1</sup>; <sup>109</sup>Pd: 36 Bq.g<sup>-1</sup>; <sup>122</sup>Sb: 13 Bq.g<sup>-1</sup>; <sup>192</sup>Ir: 10 Bq.g<sup>-1</sup>; <sup>194</sup>Ir: 650 Bq.g<sup>-1</sup>; <sup>198</sup>Au: 2.5 Bq.g<sup>-1</sup>, activity concentrations are given at the date of the TDCR measurement. Their values are very low compared to the <sup>103m</sup>Rh activity and do not induce any correction factors for the LSC measurements.

## **5. Results and discussion**

The determination of the photon emission intensities is directly linked to the sample activity measured by LSC. However, as detailed in section 3, the activity results depend on the decay scheme parameters, particularly the emission intensities of the Auger- and conversion-electrons and X-rays, and hence on the multipolarity of the gamma transition. Thus, we first determine the K X-ray intensity values from the initial activity calculation. From these values, a new data set is calculated with a new multipolarity which is used to provide an updated activity value and then the K X-ray emission intensities are calculated again. The operation is iterated until the uncertainties on the values of the new data set are compatible with the previous values.

The results for the efficiency transfer factors obtained by Monte Carlo simulations for the  $K\alpha$ ,  $K\beta$  and  $\gamma$  lines are presented in Table 4 with the associated uncertainties. These efficiency transfer factors are rather large and influence significantly the emission intensities, and their uncertainties are the main source of uncertainty on the final results.

The first results of the activity and their uncertainties are presented in Table 5. The results presented here correspond only to the  $RhCl_3$  source, since, for pure rhodium, the source activity was insufficient to determine a value with an acceptable uncertainty. The activity used for the intensity measurement is the mean of the four activity measurements:

$$A_{Rh} = 832.0 (24) \text{ kBq.g}^{-1}.$$

The first results of the emission intensities and their uncertainties are presented in Table 6.

Firstly, we note that the aim to reduce the uncertainties on the X-ray emission intensities has been achieved, since uncertainties of 2.5% have been attained, compared to earlier values between 5.5% and 7%.

Secondly, there would appear to be an inconsistency in the gamma-ray emission intensity obtained in this work,  $I_\gamma = 0.079(4)\%$ . In this simple decay scheme with only one gamma transition ( $P_\gamma = 100\%$ ), the photon emission intensities are linked to the total,  $\alpha_T$ , and partial,  $\alpha_K$ , conversion coefficients:

$$I_{XK} = \frac{\alpha_K}{1+\alpha_T} \omega_K P_\gamma \quad (\text{Eq. 3})$$

$$I_\gamma = \frac{1}{1+\alpha_T} P_\gamma \quad (\text{Eq. 4})$$

Consequently, for a pure E3 transition,  $I_\gamma$  is calculated to be 0.071(1)% and still lower for a mixing ratio including M4, since the total conversion coefficient increases (see Table 2). This

inconsistent result can be explained by the very low counting statistics under the gamma-ray full energy peak and high associated relative uncertainty (about 5%).

Thirdly, we can calculate a mixing ratio,  $E3 + 0.1\%M4$ , corresponding to the measured X-ray emission intensity results and provide a new set of conversion coefficients for the TDCR efficiency calculation. However, it appears that the activity measurement is almost independent of the mixing ratio, because the small change has a negligible effect on the TDCR detection efficiency. Therefore, no iterations are required and the K X-ray emission intensities presented in the Table 6 are the definitive results of this study. Table 7 and Figure 5 summarize the experimental values obtained in this work and compare these with other experimental values quoted in the literature. First we can observe that the most recent X-ray intensity measurements were performed more than twenty years ago and the majority of the measurements date back to the 1960-70s. The measurements are also quite dispersed and are not always consistent within their uncertainties. The intensity values obtained in this work are in good agreement with Vaninbroux and Zehner (1981) and Grunditz et al. (1969), but not with Perolat (1976) and Schötzig (1994). It is interesting to note that Vaninbroux and Zehner (1981) and Perolat (1976) measured the K X-ray emission intensities under very similar conditions, i.e. separation of the  $^{103m}\text{Rh}$  from a  $^{103}\text{Pd}$  source, an activity measurement by liquid scintillation counting and X-ray measurement with either a pressurised proportional counter (Perolat) or a Si(Li) detector (Vaninbroux and Zehner, 1981), but they obtained very different values not consistent within the uncertainties. Schötzig (1994) measured the  $^{103m}\text{Rh}$  X-ray emission intensities from the decay of  $^{103}\text{Ru}$ , where the decay scheme is extremely complicated, hence many corrections had to be taken into account.

## 6. Conclusion

Recent experimental data of K X-ray emission intensities for  $^{103\text{m}}\text{Rh}$  are uncommon. Moreover, the results are dispersed and not consistent within their uncertainties. Generally, K X-ray emission intensities were measured from the decay of  $^{103}\text{Pd}$  or  $^{103}\text{Ru}$ . In this work, we have proposed a method based on the activation of  $^{103}\text{Rh}$  by neutron inelastic scattering. The absolute K X-ray emission intensity derived in this study is  $I_{\text{XK}} = 0.0825(17)$ , and the partial  $\text{K}\alpha$  and  $\text{K}\beta$  are respectively 0.0689(17) and 0.0136(3), thus the combined relative standard uncertainties on the results are about 2-2.5%. These results are consistent with some tabulated data, despite the high disparity between them.

The value currently used to determine the activity of rhodium dosimeters in reactor dosimetry is  $I_{\text{XK}} = 0.0753(35)$  (Nucleide, 2016). With this value, the relative difference between neutron transport codes and experimental data are higher than 10% (Bourganel et al, 2015). With the new X-ray emission intensity value, the calculation and the experimental data are in much closer agreement. The result of the present study will therefore contribute to a significant improvement in reactor dosimetry.

However, it has been stated that the gamma-ray emission intensity is not compatible with the X-ray emission intensities and the multipolarity of the gamma transition. Thus, a new experiment with a high activity  $^{103}\text{Pd}$  source is planned in order to measure more accurately the gamma-ray emission intensity and to provide an additional measurement of the K X-ray emission intensities, with a different experimental approach as a complement to the present study. It is hoped that these additional experimental values will allow the Decay Data Evaluation Project (Kellett and Bersillon, 2017) to produce an evaluation of the  $^{103\text{m}}\text{Rh}$  decay scheme to provide recommended data to the users.

## References

- Agostinelli, S. et al., 2003. *Geant4 - a simulation toolkit*. Nuclear Instruments and Methods in Physics Research A506, 250-303.
- Bourganel, S. et al., 2015. *Preliminary Analysis of The FLUOLE-2 Experiment*. Proceedings of the International Conference Nuclear Energy for New Europe, NENE 2015, 404.  
<http://www.djs.si/proc/nene2015/htm/proceedings.htm>
- Bresemi, A.M., Bresemi, M., Neumann, H., 1967. *Measurement of K X-Ray Emission in the Decay of  $^{103m}\text{Rh}$* . Journal of Inorganic and Nuclear Chemistry, 29, 15-20.
- Campbell, J.L., Papp, T., 2001. *Widths of the atomic K-N7 levels*. Atomic Data and Nuclear Data Tables 77, 1–56.
- Cassette, P., Vatin, R., 1992. *Experimental evaluation of TDCR models for the 3 PM liquid scintillation counter*. Nuclear Instruments and Methods in Physics Research A312, 95-99.
- Czock, K.H., Haselberger, N., Reichel, F. 1975. *The disintegration of  $^{103m}\text{Rh}$* . International Journal of Applied Radiation and Isotopes, 26, 417-421.
- JCGM, 2008. *Evaluation of measurement data — Supplement 1 to the “Guide to the expression of uncertainty in measurement” — Propagation of distributions using a Monte Carlo method*. JCGM 101: 2008.
- Grunditz, Y. et al., 1969. *Studies in the Decay of  $^{103}\text{Pd}$* . Nuclear Physics A133 (2), 369-384.
- Ing, H., Cross, W.G., 1973. *Absolute counting of K X-rays from  $^{103}\text{Rh}$  in thick foils*. The International Journal of Applied Radiation and Isotopes, Volume 24 (8) 437-450.
- Kellett, M.A., Bersillon, O. 2017. *The Decay Data Evaluation Project (DDEP) and the JEFF-3.3 radioactive decay data library: Combining international collaborative efforts on evaluated decay data*. EPJ Web of Conferences 146, 02009.
- Kibédi, T. et al., 2008. *Evaluation of theoretical conversion coefficients using BrIcc*. Nuclear Instruments and Methods in Physics Research A589 (2), 202-229.

Live Chart of Nuclides 2017, <https://www-nds.iaea.org/relnsd/vcharthtml/VChartHTML.html>

Nucleide 2016, [http://www.nucleide.org/DDEP\\_WG/DDEPdata.htm](http://www.nucleide.org/DDEP_WG/DDEPdata.htm)

Perolat, J.P. et al., 1976. *Etude du schéma de désintégration du  $^{103m}\text{Rh}$* . Note technique LMRI 76-13.

Ruellan H. et al., 1996. *A new spectra processing code applied to the analysis of  $^{235}\text{U}$  and  $^{238}\text{U}$  in the 60 to 200 keV energy range*. Nuclear Instruments and Methods in Physics Research A369, 651-656.

Salvat, F., Fernandez-Varea, J.-M., Sempau, J., 2015. *PENELOPE-2014: A Code System for Monte Carlo Simulation of Electron and Photon Transport*. OECD NEA Data Bank.

Santamarina, A. et al., 2009. *The JEFF-3.1.1 Nuclear Data Library - Validation Results from JEF-2.2 to JEFF-3.1.1* - JEFF Report 22, OECD NEA Data Bank.

Santry, D.C., Butler, J.P., 1974. *Cross Section Measurements for the  $^{103}\text{Rh}(n,n')^{103m}\text{Rh}$  Reaction from 0.122 to 14.74 MeV*. Canadian Journal of Physics 52(15), 1421-1428.

Schötzig, U., 1994. *Photon emission probabilities in the decay of  $^{103}\text{Ru}^{103m}\text{Rh}$* . Applied Radiation and Isotopes, 45(6) 641-644.

Vaninbroukx, R., Zehner, W., 1981. *Determination of the KX-ray emission probability in the decay of  $^{103m}\text{Rh}$* . International Journal of Applied Radiation and Isotopes, 32 (11), 850.

Vuorinen, A. (1967). *Calibration of  $^{103m}\text{Rh}$  by the coincidence method*. Proceedings of a symposium on standardization of radionuclides (10-14 October 1966) IAEA, 1967, 257-262.

Zsolnay, E.M. et al., 2012. *Summary Description of the New International Reactor Dosimetry and Fusion File (IRDF release 1.0)*. International Nuclear Data Committee, INDC(NDS)-

0616

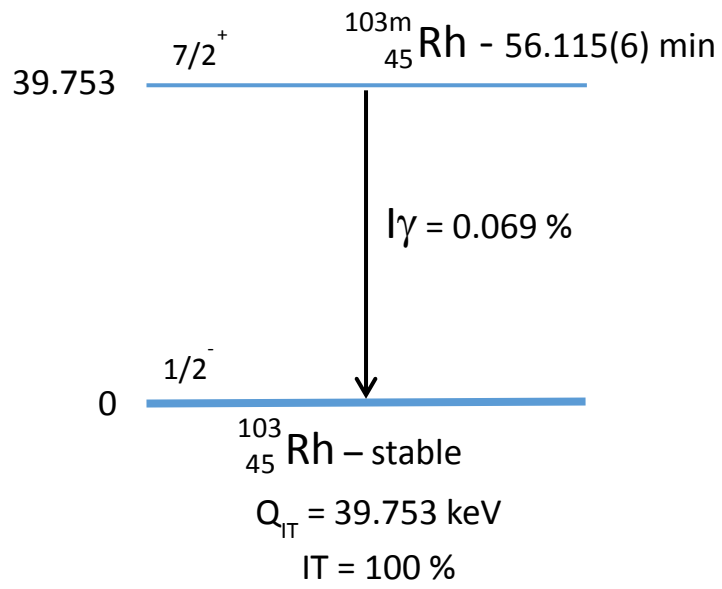


Figure 1:  $^{103m}\text{Rh}$  decay scheme.

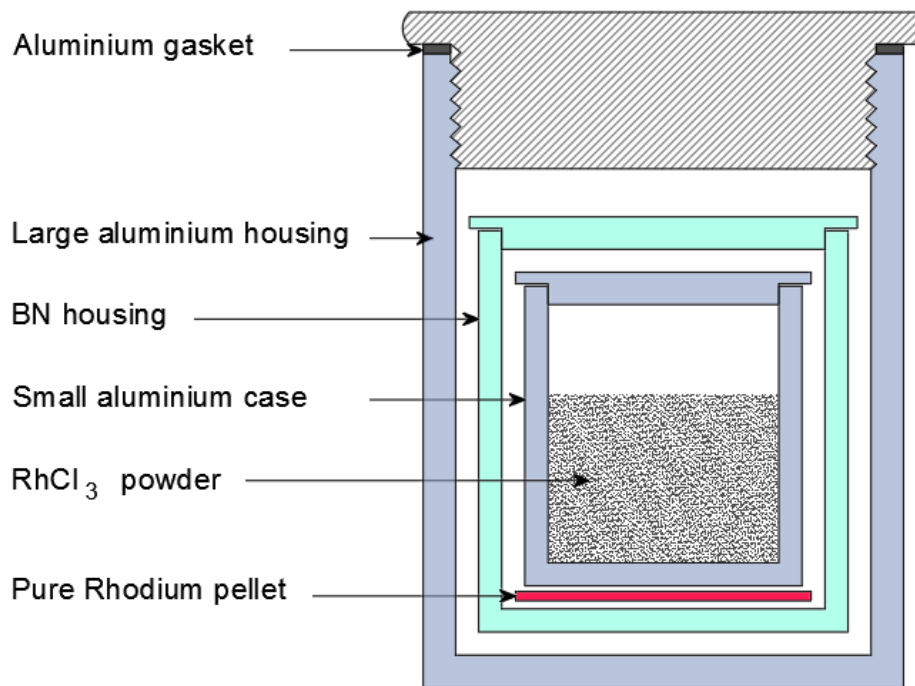


Figure 2: Conditioning of the rhodium samples for irradiation.

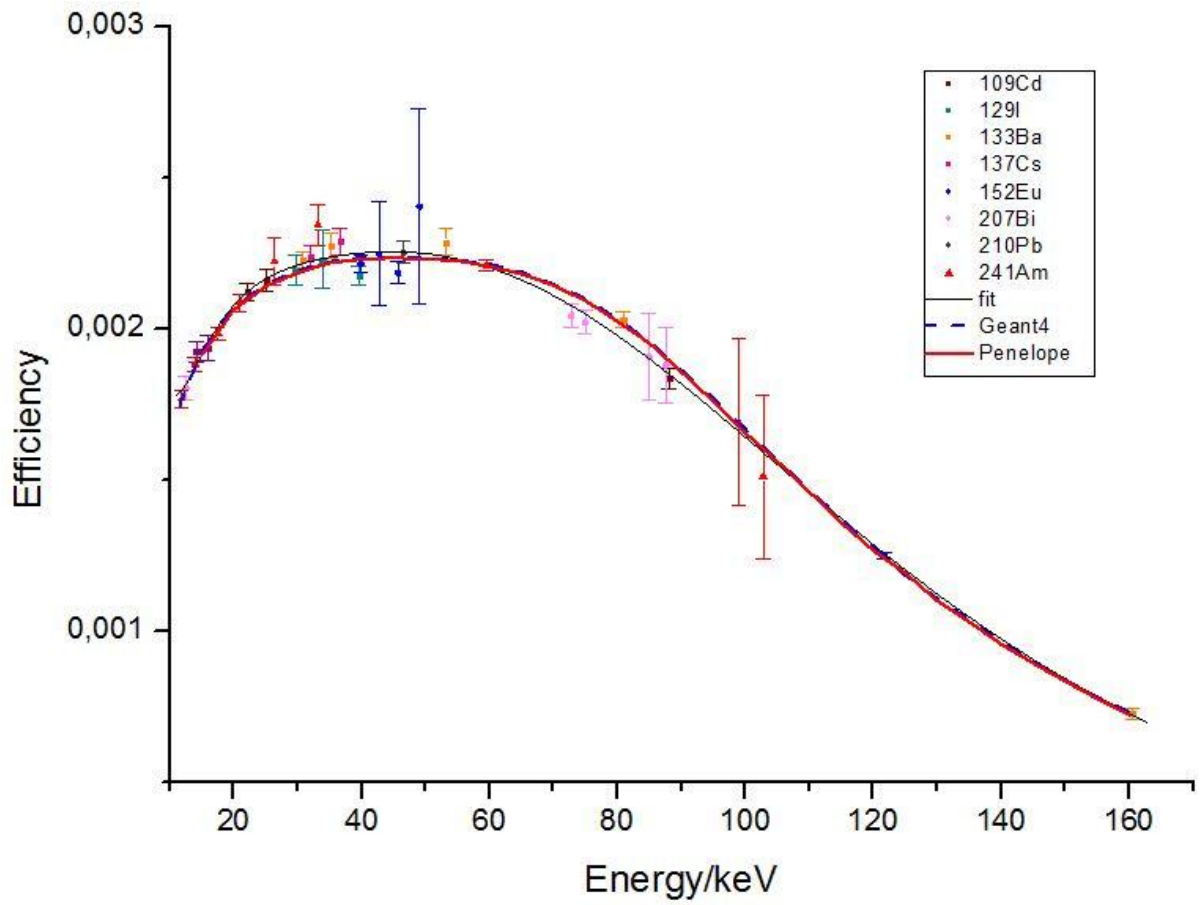


Figure 3: Experimental efficiency calibration of the HPGe detector for point sources at 7.8 cm from the detector window. Black line: fit of experimental values; red line: Penelope results; dotted blue line: Geant4 results.

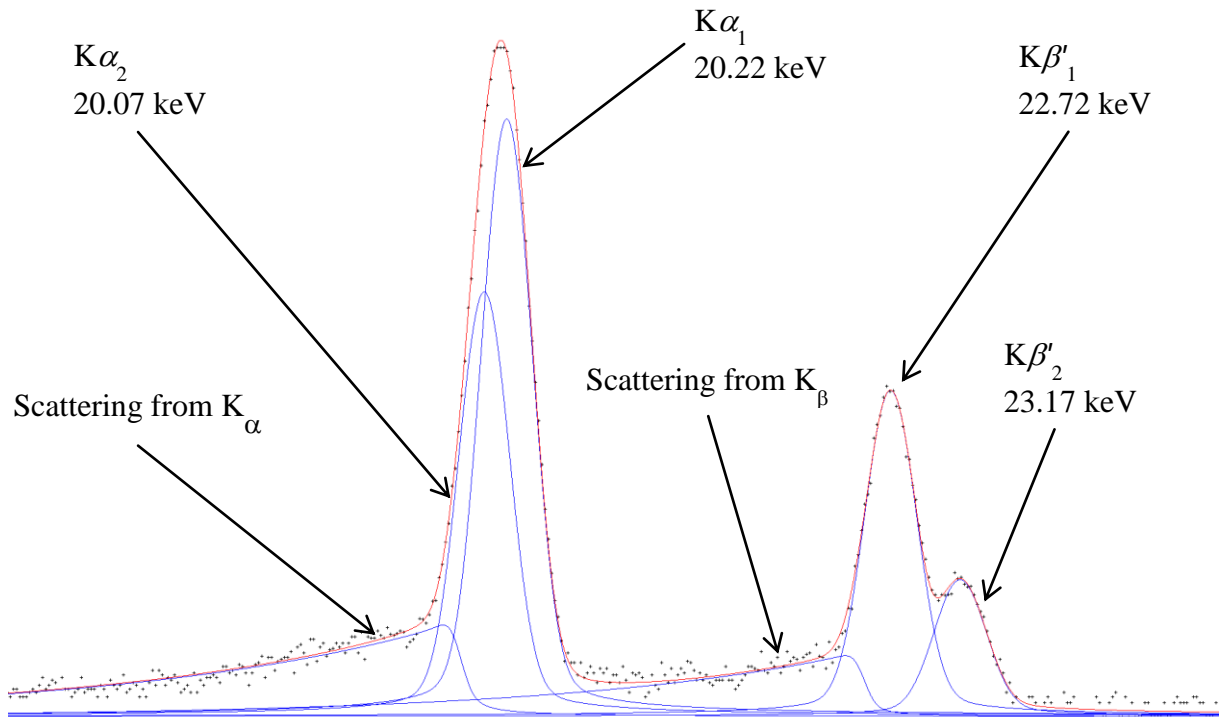


Figure 4: Example of peak processing using COLEGRAM.

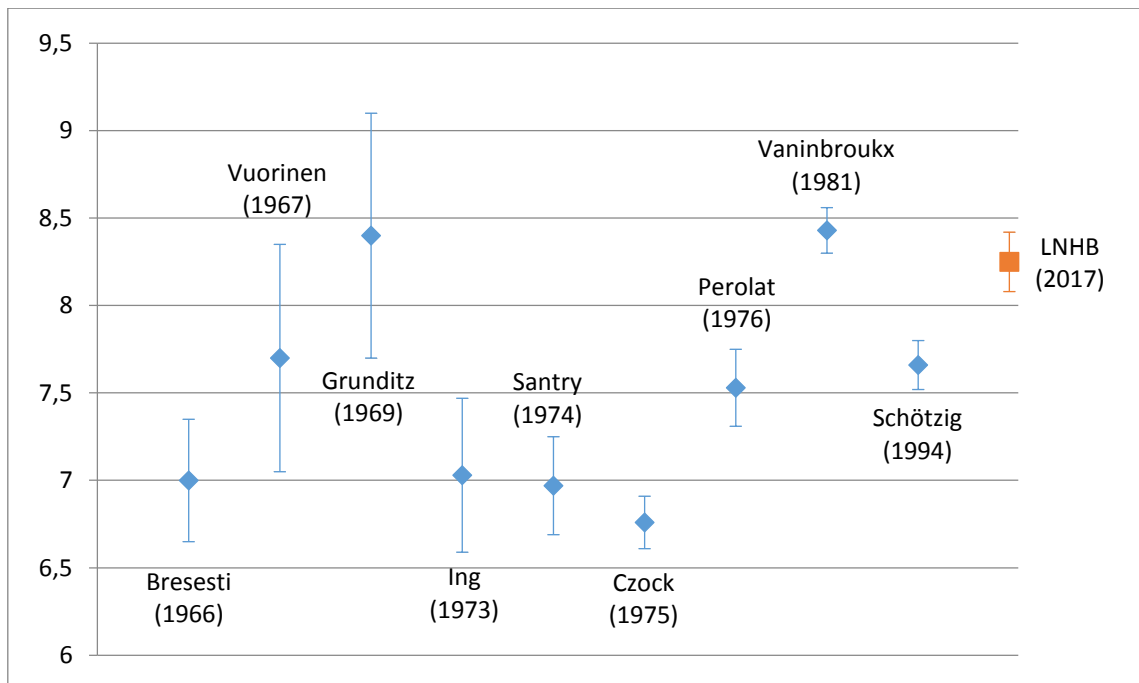


Figure 5: Comparison of experimental values of K X-ray photon emission intensities in the decay of  $^{103m}\text{Rh}$ .

Table 1 : Energy and intensities of the electron and K X-ray emissions.

	Energy (keV)	Electrons (per 100 disint.)		Energy (keV)	Photons (per 100 disint.)
$e_{AL}$	1.7 - 3.0	78.6 (5)	XL	2.3702 - 3.3663	4.08 (9)
$e_{AK}$					
KLL	16.286 - 17.097		$XK\alpha_2$	20.074	2.25 (6)
KLX	19.138 - 20.214	1.86 (8)	$XK\alpha_1$	20.216	4.27 (9)
KXY	21.966 - 23.215				
$ec_T$	16.536 - 39.754	99.912 (1358)	$XK'\beta_1$	22.699 - 22.914	1.161 (35)
$ec_K$	16.536 (6)	9.73 (26)	$XK'\beta_2$	23.173 - 23.217	0.190 (9)
$ec_L$	36.344 - 36.752	73.1 (13)			
$ec_M$	39.129 - 39.449	14.90 (29)			
$ec_{N+}$	39.675 - 39.754	2.182 (43)			

Table 2: Comparison of the data obtained with two multiplicities (E3 and E3 + 0.05%M4) for the 39.756 keV gamma-transition in  $^{103m}\text{Rh}$ .  $P_{eci}$  is the conversion probability of an electron in the  $i$  shell and  $\alpha_i$  corresponds to the internal conversion coefficient in the  $i$  shell.

Rh-103m	Data					
	E3	uabs	E3 + 0,05%M4	uabs	difference	u diff
PecK	0.0963	0.0014	0.0983	0.0035	-0.0020	0.0037
PecL	0.732	0.011	0.730	0.015	0.0023	0.0190
PecM	0.1489	0.0021	0.1492	0.0035	-0.0003	0.0041
PecN+	0.02180	0.00036	0.02184	0.00049	0.0000	0.0006
$\alpha_K$	135.2	1,9	141	5		
$\alpha_L$	1028	15	1047	22		
$\alpha_M$	209	3	214	5		
$\alpha_{N+}$	30.61	0.5	31.3	0.7		
$\alpha_T$	1403	15	1433	23		

Table 3: Comparison between the germanium crystal data provided by the manufacturer and the data used for MC simulations. *Dead-layer* corresponds to the dead layer at the entrance of the crystal and *Inactive crystal* is the dead layer at the exit of the crystal.

	Supplier data	Current data for MC simulations
Ge crystal diameter (mm)	16	15.44
Ge active crystal diameter (mm)	16	15.1
Ge crystal thickness (mm)	10	11.1
Active crystal thickness (mm)	9.4	6.7
Inactive crystal thickness (mm)	0.6	4.4
Dead-layer thickness ( $\mu\text{m}$ )	0.3	0.8
Be window-detector distance (mm)	7	8.21

Table 4: Efficiency transfer factors from point sources to volume sources obtained by Monte Carlo simulation.

Photon type and energy (keV)	Efficiency transfer factor	Absolute uncertainties (k=1)	Relative uncertainty (%)
K $\alpha$ : 20.167	3.35	0.07	1.94
K $\beta$ : 22.781	2.85	0.05	1.81
$\gamma$ : 39.756	2.77	0.05	1.74

Table 5: Results of the RhCl<sub>3</sub> powder activity measurement by liquid scintillation counting

Source	Count rate (s <sup>-1</sup> .g <sup>-1</sup> )	Detection efficiency	Standard deviation of detection efficiency	A (Bq.g <sup>-1</sup> )	Standard deviation	Relative uA
1	757 734	0.9134	0.0021	829 575.213	1 908.023	0.23%
2	761 352	0.9147	0.0021	832 351.591	1 914.409	0.23%
3	758 555	0.913	0.0021	830 837.897	1 910.927	0.23%
4	764 102	0.9149	0.0021	835 175.429	1 920.903	0.23%
Mean				831 985.033	2 410.818	0.29%

Table 6: Photon emission intensities in the decay of <sup>103m</sup>Rh

	Emission intensity	Absolute uncertainty (k=1)	Relative uncertainty
X K $\alpha$	0.0689	0.0017	2.5%
X K $\beta$	0.0136	0.0003	2.5%
X K <sub>tot</sub>	0.0825	0.0017	2.1%
$\gamma$	0.00079	0.00004	4.8%

Table 7: Measurement results of  $^{103\text{m}}\text{Rh}$  K X-ray emission intensities

Authors	Emission intensity	Absolute uncertainty
Breesti (1966)	7.00	0.35
Vuorinen (1967)	7.70	0.65
Grunditz (1969)	8.4	0.7
Ing (1973)	7.03	0.44
Santry (1974)	6.97	0.28
Czock (1975)	6.76	0.15
Perolat (1976)	7.53	0.22
Vaninbroukx (1981)	8.43	0.13
Schötzig (1994)	7.66	0.14
<b>Present study (2017)</b>	<b>8.25</b>	<b>0.17</b>